Applied Physics Letters

Frequency response of large aperture oxide-confined 850 nm vertical cavity surface emitting lasers

Cite as: Appl. Phys. Lett. **95**, 131101 (2009); https://doi.org/10.1063/1.3231446
Submitted: 26 July 2009 • Accepted: 26 August 2009 • Published Online: 28 September 2009

A. Mutig, S. A. Blokhin, A. M. Nadtochiy, et al.

Frequency response of large aperture oxide-confined 850 nm vertical cavity surface emitting lasers

A. Mutig,[1,a)] S. A. Blokhin,[1,b)] A. M. Nadtochiy,[1,b)] G. Fiol,[1] J. A. Lott,[2] V. A. Shchukin,[2] N. N. Ledentsov,[2] and D. Bimberg[1]
[1]*Institut für Festkörperphysik und Zentrum für Nanophotonik, Technische Universität Berlin, Hardenbergstrasse 36, 10623 Berlin, Germany*
[2]*VI Systems GmbH, Hardenbergstrasse 7, 10623 Berlin, Germany*

(Received 26 July 2009; accepted 26 August 2009; published online 28 September 2009)

Small and large signal modulation measurements are carried out for 850 nm vertical cavity surface emitting lasers (VCSELs). The resonance frequency, damping factor, parasitic frequency, and *D*-factor are extracted. Small signal modulation bandwidths larger than 20 GHz are measured. At larger currents the frequency response becomes partially limited by the parasitics and damping. Our results indicate that by increasing the parasitic frequency, the optical 3 dB bandwidth may be extended to ~25 GHz. A decrease in the damping should enable VCSEL bandwidths of 30 GHz for current densities not exceeding ~10 kA/cm^2 and ultimately error-free optical links at up to 40 Gbit/s. © *2009 American Institute of Physics*. [doi:10.1063/1.3231446]

The forecast for the serial transmission speeds used for data bit communication links is a continued exponential increase with time, directly in concert with silicon integrated circuit scaling and in response to human society's perpetual hunger for massive increases in bandwidth. As a result, the fundamental electromagnetic limitations of copper-wire-based links at bit rates of >10 Gbit/s and at distances of >1 m make fiber based optics for data communication indispensable. Vertical cavity surface emitting lasers (VCSELs) are key devices for very short reach applications in fiber-optic networks and active optical cables.[1] The 850 nm VCSELs are particularly important since they are already used in local area and storage area networks applications and are expected to play an increasingly important role in future optical standards. In the past few years great progress in the area of high-speed VCSELs at different wavelengths has been achieved. Data transmission at bit rates of 32 Gbit/s (850 nm),[2] 35 Gbit/s (980 nm),[3] and 22 Gbit/s (1550 nm)[4] has been demonstrated. Very recently 850 nm VCSELs exhibiting error-free operation up to 20 Gbit/s[5]) and 40 Gbit/s[6] were reported.

In order to understand better and further improve VCSEL performance, it is very important to understand the physical processes inside the devices and to analyze important laser parameters such as damping factor, resonance frequency, and parasitic cut-off frequency. For this purpose small signal modulation response (S_{21}) and microwave reflection (S_{11}) measurements were carried out for two oxide-confined 850 nm VCSELs[6] with aperture diameters of 6 and 9 μm at room temperature.

The VCSEL structures were grown on a semi-insulated (SI) GaAs substrate using metal-organic vapor-phase epitaxy. They consist of 23/35.5 top/bottom GaAlAs doped distributed Bragg reflectors with linear compositional gradings, a GaAlAs-based microcavity and multiple strained InGaAs insertions as the active region. Selective wet oxidation of Al(Ga)As materials[7] was applied to create lateral confinement for the injected current and optical field. Planarization with bisbenzocyclobutene was applied to reduce the parasitic capacitance of the ground-source-ground (GSG) contact pads and for ease of on-wafer high-frequency probing. While small mesa diameters and deep mesa etching are needed to reduce electrical parasitics, from the thermal point of view rather larger mesas and shallow etching are preferable. Higher doping levels reduce resistance of the devices but also increase absorption loss. Small oxide aperture diameters reduce mode volume and threshold current, and this improves the high-speed performance of the lasers but also increases current density and decreases output power. Thus the overall design incorporating a rather complex compromise for several competing factors such as high modulation speed, high thermal conductivity, large output power, and low current density was applied.

The light-current-voltage characteristics of the two investigated VCSELs are shown in Fig. 1. The threshold currents are 330 and 590 μA for the 6 and 9 μm VCSELs, respectively. The maximum differential efficiency for both devices is ~60%. The maximum output power is larger than 5 mW for the 6 μm VCSEL and larger than 9 mW for the 9 μm VCSEL. The differential resistance of the 6 μm VCSEL is ~110 Ω at 5 mA and for the 9 μm VCSEL is ~90 Ω at 9 mA.

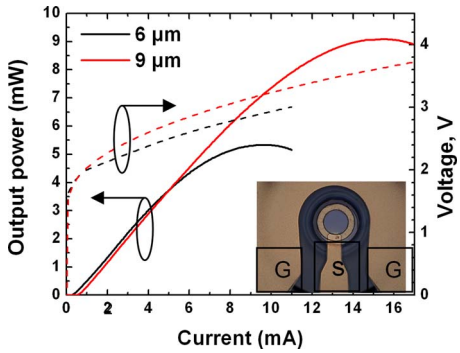

FIG. 1. (Color online) Light-current-voltage characteristics of the VCSELs with 6 and 9 μm aperture diameters. The inset shows a visible-light microscope image of an example processed VCSEL in the GSG configuration.

a)Electronic mail: mutig@sol.physik.tu-berlin.de.
b)On leave from the Saint-Petersburg Physical Technological Centre for Research and Education of the Russian Academy of Sciences, Khlopina 8/3, Saint-Petersburg, 194021 Russian Federation.

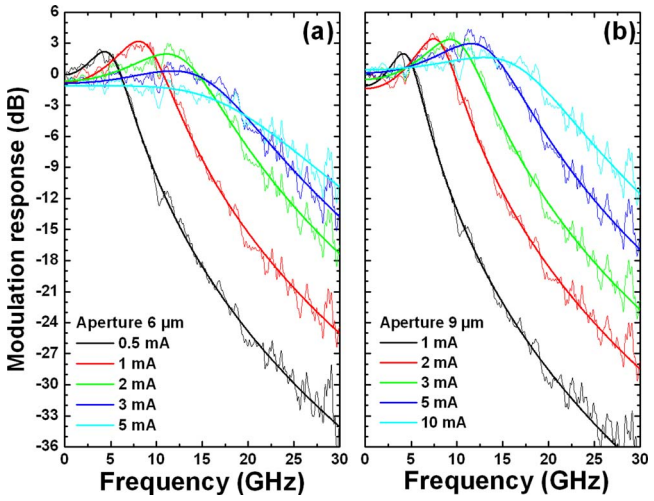

FIG. 2. (Color online) Magnitude of the small signal modulation response S_{21} for different applied bias currents and the corresponding fits for the VCSELs with 6 μm (a) and 9 μm (b) oxide aperture diameters.

The small signal modulation response and scattering parameters were measured using a network analyzer and a calibrated photodetector in the range from 50 MHz to 30 GHz. The extraction procedure of the physical parameters was similar to that described in[8] and was as follows. At the beginning, the measured optical small signal modulation response (S_{21}) was corrected for the response of the photodetector. Then, using the equivalent circuit model described in,[9] the parasitic resistances and capacitances inside of the VCSEL were extracted by fitting the circuit model to the measured microwave reflection curves (S_{11}). After that, using the values for the parasitic elements and the equivalent circuit model, the parasitic low pass curve for the electrical microwave transmission was calculated and subtracted from the calibrated measured optical data. Finally the resonance frequency f_R and damping factor γ were extracted using the first part of the theoretical rate Eq. (1) without the parasitic low pass. This method of data extraction has several advantages as compared to methods that fit only the S_{21} curve data to Eq. (1). First the use of more experimental information (here the measured S_{21} and S_{11} curves) minimizes the error of the extracted parameters. The second advantage is that one is not limited by the first order low pass response of the form found in the second part of the Eq. (1) with the parasitic cut-off frequency f_P. Instead the calculated form of the parasitic low pass response based on the parameters extracted from the measured S_{11} data is used, and this makes the fits more exact,

$$H(f) = f_R^2 \left(f_R^2 - f^2 + jf\frac{\gamma}{2\pi} \right) \left(1 + j\frac{f}{f_P} \right). \quad (1)$$

The measured small signal modulation response curves with corresponding fits for different currents at room temperature are shown in Fig. 2 for 6 and 9 μm VCSELs, respectively. All fits show excellent agreement with the measured data. The maximum 3 dB frequency for both devices is larger than 20 GHz at 5 and 10 mA for the 6 and 9 μm VCSELs, respectively. The S_{21} curves slightly differ for both cases. While in the case of the 6 μm VCSEL, the modulation response curve at 5 mA is damped; the 9 μm VCSEL shows a resonance of $\sim$1 dB at 10 mA. This result indicates that the high-speed performance of the 6 μm VCSEL is at least partially limited by damping. Small signal modulation bandwidths of 21 and 24 GHz has been demonstrated in the past for VCSELs with oxide-confined apertures of 4 μm diameter and emitting at 850 nm[10] and 1100 nm, where the latter device is based on a buried tunnel junction.[11] The bandwidths measured here are only slightly lower than these record values.

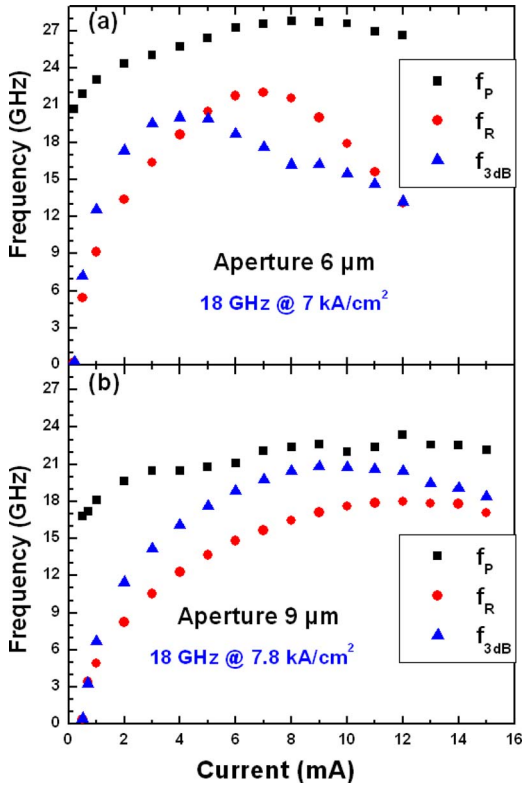

FIG. 3. (Color online) Parasitic cut-off (black), resonance (red), and 3 dB (green) frequencies for the VCSELs 6 μm (a) and 9 μm (b) apertures.

Figure 3 shows the parasitic cut-off frequencies f_P, resonance frequencies f_R, and the 3 dB frequencies $f_{3\ \mathrm{dB}}$ extracted from the S_{21} and S_{11} measurements for both devices. For both VCSELs the parasitic cut-off frequencies are, as expected, larger than the 3 dB frequencies. The parasitic f_P are not limiting the speed of the VCSELs at low currents, and the 3 dB frequencies significantly exceed the resonance frequency. We note that the dependence of the cut-off frequency of the electrical parasitics at low currents is due to the current dependence of the resistances and capacitances inside the device. Parasitic cut-off frequencies larger than 27 GHz for the 6 μm VCSEL and 23 GHz for the 9 μm VCSEL are extracted and indicate a noticeable impact of the parasitics on the high-speed performance at large currents. The resonance frequency for the 6 μm oxide-diameter VCSEL at currents larger than 5 mA is higher than the 3 dB frequency, showing that the device is mainly limited by damping, as one is able to conclude from the data in Fig. 2. In the case of the 9 μm oxide-diameter, VCSEL the resonance frequency is smaller than the 3 dB frequency, showing here a stronger impact of thermal roll-over. We note that 3 dB bandwidths close to $\sim$20 GHz are realized at current densities of only $\sim 7-8$ kA/cm^2. This result is particularly striking for the 6 μm oxide aperture VCSEL, as the reliability of small aperture oxide-confined VCSELs is typically much better compared than that of their large aperture counterparts for equal current densities.[12] It was previously be-

lieved however that much higher current densities are needed for these devices to reach even 10 Gb/s bit rates since the data transfer rate increases roughly with the square root of current density.

Resonant frequencies of up to 22 GHz are recorded (Fig. 3). At lower currents the impact of parasitics and damping is small, and the 3 dB bandwidth exceeds the resonance frequency by a factor of ~1.4. At current densities of ~7 kA/cm^2, the optical 3 dB bandwidth approaches 18 GHz, while the frequency response becomes partially affected by the parasitic bandwidth of 23 and 27 GHz for the larger and smaller oxide-aperture devices, respectively. The resonant feature in the frequency response curve of the 6 μm VCSEL becomes severely damped. With a further increase in the parasitic frequency and a decrease in the damping, assuming that the 1.4 ratio is maintained, the optical 3 dB bandwidths are expected to reach 30 GHz for otherwise similar device parameters and current densities of ~10 kA/cm^2.

By fitting a linear function to the extracted squared resonance frequencies as a function of the current, one can extract the important *D*-factor, which yields internal laser parameters such as differential gain and mode volume.[9,13] The extracted *D*-factors for the 6 and 9 μm VCSELs are 9.8 and 6.5 GHz/$\sqrt{}$mA, respectively. As one would expect from theory, the *D*-factor should decrease with increasing mode volume and due to the square root dependence is inversely proportional to the diameter of the active region. In fact dividing the *D*-factor of 9.8 GHz/$\sqrt{}$mA for the 6 μm VCSEL by the *D*-factor of 6.5 GHz/$\sqrt{}$mA for the 9 μm VCSEL gives 1.51, identical to the aperture diameter ratio of 9:6=1.5. Clearly our analysis is consistent not only for one particular device but also for the entire set of devices.

To extract the *K*-factor yielding the damping limit of the speed, one must fit the damping as a function of the squared resonance frequency.[9,13] Here the damping shows a weak superlinear behavior because of heating. A similar observation in 850 nm VCSELs was recently reported,[13] and this observed behavior makes extraction of the exact value of the *K*-factor difficult. Values between 0.23 and 0.38 ns can be extracted for both devices depending on the fitting procedure. Nevertheless one can compare the damping factor values γ of the two lasers, and in this study these terms are essentially equal.

Large signal modulation experiments were carried out for the 6 μm VCSEL using a nonreturn to zero (NRZ) data pattern with a (2^7-1) pseudorandom bit sequence (PRBS) in the back-to-back configuration (BTB, ~3 m fiber). In Fig. 4 the optical eye diagrams for different bit rates and currents with corresponding signal-to-noise ratios (SNR) are shown. All eyes are clearly open. For the top two eye diagrams at 20 Gbit/s and at different currents of 3 and 5 mA, the SNRs are 5.8 and 7.1 as shown. The current of 3 mA corresponds for 6 μm aperture diameter VCSEL to a current density of ~10.6 kA/cm^2, i.e., a value sufficiently low to ensure reliable operation. The eye at 25 Gbit/s has a SNR of 6.7, and at 30 Gbit/s we observe a SNR of 5.3. The deconvoluted VCSEL rise time is found to be <10 ps and remains temperature insensitive up to 100 °C.[6]

To conclude we have carried out a comparative small signal modulation analysis at room temperature for two otherwise identical VCSELs with different oxide-confined aperture diameters of 6 and 9 μm. The results show that a further reduction in parasitics and damping improves the optical 3 dB bandwidth up to and beyond ~30 GHz. Although eye diagrams with SNRs above five at up to 30 Gbit/s were demonstrated, the SNRs remain limited by our present test setup.

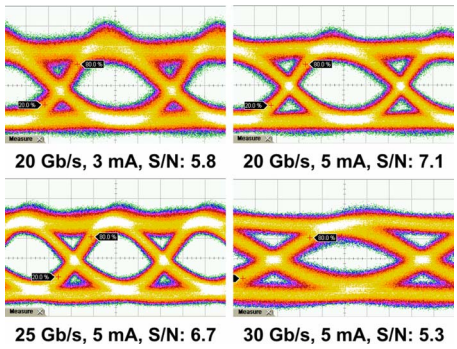

FIG. 4. (Color online) Eye diagrams for the VCSEL with 6 μm aperture at different bit rates and currents in a BTB configuration with (2^7-1) PRBS NRZ.

This work was supported in different parts by the German Ministry for Education and Research bmb+f (NanOp), the Deutsche Forschungsgemeinschaft (Grant No. Sfb 787), the State of Berlin (100×100 Optics), the European Community's Seventh Framework Programme (Grant No. FP7/2007-2013, VISIT), St. Petersburg Scientific Centre RAS, the Program of Fundamental Studies of the Presidium RAS, and the Russian Federal Agency of Education.

[1] D. Collins, N. Li, D. Kuchta, F. Doany, C. Schow, C. Helms, and L. Yang, Proc. SPIE **6908-6909**, 690809 (2008).
[2] P. Westbergh, J. S. Gustavsson, A. Haglund, A. Larsson, F. Hopfer, D. Bimberg, and A. Joel, Electron. Lett. **45**, 366 (2009).
[3] Y.-C. Chang, C. S. Wang, and L. A. Coldren, Electron. Lett. **43**, 1022 (2007).
[4] W. Hofmann, M. Müller, A. Nadtochiy, C. Meltzer, A. Mutig, G. Böhm, J. Rosskopf, D. Bimberg, M.-C. Amann, and C. Chang-Hasnain, Opt. Express **17**(20), 17547 (2009).
[5] J. A. Lott, V. A. Shchukin, N. N. Ledentsov, A. Stintz, F. Hopfer, A. Mutig, G. Fiol, D. Bimberg, S. A. Blokhin, L. Y. Karachinsky, I. I. Novikov, M. V. Maximov, N. D. Zakharov, and P. Werner, *20 Gbit/s error free transmission with ~850 nm GaAs-based vertical cavity surface emitting lasers (VCSELs) containing InAs-GaAs submonolayer quantum dot insertions* Proceedings of SPIE 7211, paper 721114, Photonics West, San Jose, CA, 29 January 2009.
[6] S. A. Blokhin, J. A. Lott, A. Mutig, G. Fiol, N. N. Ledentsov, M. V. Maximiv, A. M. Nadtochiy, V. A. Shchukin, and D. Bimberg, Electron. Lett. **45**, 501 (2009).
[7] V. A. Haisler, F. Hopfer, R. L. Sellin, A. Lochmann, K. Fleischer, N. Esser, W. Richter, N. N. Ledentsov, D. Bimberg, C. Möller, and N. Grote, Appl. Phys. Lett. **81**, 2544 (2002).
[8] Y.-C. Chang and L. A. Coldren, IEEE J. Sel. Top. Quantum Electron. **15**, 704 (2009).
[9] A. Mutig, G. Fiol, K. Pötschke, P. Moser, D. Arsenijevic, V. A. Shchukin, N. N. Ledentsov, S. S. Mikhrin, I. L. Krestnikov, D. A. Livshits, A. R. Kovsh, F. Hopfer, and D. Bimberg, IEEE J. Sel. Top. Quantum Electron. **15**, 679 (2009).
[10] K. L. Lear, V. M. Hietala, H. Q. Hou, M. Ochiai, J. J. Banas, B. E. Hammons, J. Zolper, and S. P. Kilcoyne, *Advances in Vertical Cavity Surface Emitting Lasers*, OSA Trends in Optics and Photonics, Vol. 15 (Optical Society of America, Washington, D.C., 1997), pp. 69–74.
[11] T. Anan, N. Suzuki, K. Yashiki, K. Fukatsu, H. Hatakeyama, T. Akagawa, K. Tokutome, and M. Tsuji, International Symposium on VCSELs Integrated Photonics, Tokyo, Japan, 17–18 Dec. 2007, pp. 76–78.
[12] B. M. Hawkins, R. A. Hawthorne, J. K. Guenter, J. A. Tatum, and J. R. Biard, Proceedings of the 52nd Electronic Components and Technology Conference, 2002, pp. 540–550.
[13] P. Westbergh, J. S. Gustavsson, A. Haglund, M. Sköld, A. Joel, and A. Larsson, IEEE J. Sel. Top. Quantum Electron. **15**, 694 (2009).